Article

Cu, Fe, or Ni doped molybdenum oxide supported on Al_2O_3 for the oxidative dehydrogenation of ethylbenzene

Tiago Pinheiro Braga [a],*, Antônio Narcísio Pinheiro [c], Edson R. Leite [c], Regina Cláudia R. dos Santos [b], Antoninho Valentini [b]

[a] LABPEMOL-Laboratório de Peneiras Moleculares, Institute of Chemistry, Federal University of Rio Grande do Norte, Natal, RN, CEP: 59078-970, Brazil
[b] Langmuir-Laboratório de Adsorção e Catálise, Department of Analytical Chemistry and Physical Chemistry, Federal University of Ceará, Fortaleza, CE, CEP:60440-554, Brazil
[c] Department of Chemistry, Federal University of São Carlos, São Carlos, SP, CEP:13560-905, Brazil

ARTICLE INFO

ABSTRACT

Molybdenum-based catalysts supported on Al_2O_3 doped with Ni, Cu, or Fe oxide were synthesized and used in ethylbenzene dehydrogenation to produce styrene. The molybdenum oxide was supported using an unconventional route that combined the polymeric precursor method (Pechini) and wet impregnation on commercial alumina. The samples were characterized by X-ray diffraction (XRD), N_2 adsorption-desorption isotherms, temperature-programmed reduction of H_2 (H_2-TPR), and thermogravimetric (TG) analysis. XRD results showed that the added metals were well dispersed on the alumina support. The addition of the metal oxide (Ni, Cu, or Fe) of 2 wt% by wet impregnation did not affect the texture of the support. TPR results indicated a synergistic effect between the dopant and molybdenum oxide. The catalytic tests showed ethylbenzene conversion of 28%–53% and styrene selectivity of 94%–97%, indicating that the addition of the dopant improved the catalytic performance, which was related to the redox mechanism. Molybdenum oxides play a fundamental role in the oxidative dehydrogenation of ethylbenzene to styrene by its redox and acid–base properties. The sample containing Cu showed an atypical result with increasing conversion during the reaction, which was due to metal reduction. The Ni-containing solid exhibited the highest amount of carbon deposited, shown by TG analysis after the catalytic test, which explained its lower catalytic stability and selectivity.

1. Introduction

Styrene is the main product used in the manufacture of materials such as plastic, rubber, resins, and intermediates in organic synthesis. The main route for the production of styrene is the dehydrogenation of ethylbenzene in the presence of water vapor (the current industrial process) described in Eq. (1):

$$C_8H_{10} \text{ (g)} \rightleftharpoons H_2 \text{ (g)} + C_8H_8 \text{ (g)} \qquad (1)$$
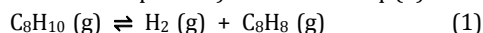
In this process, the most common catalysts used industrially are based on iron oxide (hematite) and contain various promoters such as potassium oxide, chromium, cerium, among others [1,2].

On the other hand, ethylbenzene dehydrogenation in the presence of CO_2 (Eq. (2)) has aroused considerable interest because the process with CO_2 requires less energy compared to the water vapor system.

$$C_8H_{10} \text{ (g)} + CO_2 \text{ (g)} \rightleftharpoons C_8H_8 \text{ (g)} + CO \text{ (g)} + H_2O \text{ (g)} \quad (2)$$
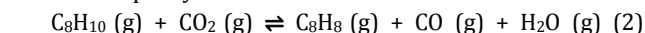
Furthermore, considering that CO_2 contributes to the green-

house effect, this alternative process can provide a commercial application of CO_2 as a soft oxidant [3–11].

The literature reports several methods for the synthesis and different compositions for the preparation of catalysts for the dehydrogenation of ethylbenzene in the presence of CO_2 [12–14]. Most of these studies used iron oxide (hematite) supported on Al_2O_3 or silicon. However, these materials are deactivated during the reaction, which is associated with the partial reduction of the hematite leading to the formation of magnetite. In addition, the deposition of carbon on the solid surface directly affects the conversion, selectivity, and catalyst stability [15]. Thus, finding alternatives to iron oxide that can be used under the drastic reaction conditions remains a challenge for this process [16–18]. Progress in the research of ethylbenzene dehydrogenation is mainly on the disadvantages of the commercial processes, catalyst deactivation, and environmental aspects as presented in several review articles [19–23].

Among the different materials studied, molybdenum oxide is considered promising because it gives a high activity, selectivity, and stability in this reaction [16–18]. Wong et al. [16] conducted a study of catalysts based on iron oxide and molybdenum oxide supported on MCM-41 and amorphous silica. They proposed that the interconnected defects of tubular MCM-41 provided better transport of reactant and product in the catalytic reaction, leading to better catalytic performance. In addition, molybdenum oxide exhibited catalytic activity higher than the iron oxide solids. Thus, these results demonstrated that catalysts based on molybdenum oxide could be an interesting alternative in ethylbenzene dehydrogenation.

Morán et al. [17] synthesized catalysts containing Pt, Mo, and Pt-Mo using clay as the support. These materials showed high catalytic activity in ethylbenzene dehydrogenation, which was attributed to the high thermal stability and high surface area of the support allowing a high dispersion of the metallic phase. The reduced catalysts presented higher activity than the unreduced solids.

Moronta et al. [18] studied the catalytic behavior of bimetallic catalysts containing Co and Mo supported on natural clays. These materials were tested in their reduced and unreduced form for ethylbenzene dehydrogenation. The reduced catalysts were more active than the unreduced solids. The low activity of all the catalysts was attributed to the low surface area of the support, which resulted in a low metal dispersion. It was observed that the low dispersion of the molybdenum oxide on the surface of the support was responsible for the low activity of these materials in this reaction. Hence, the development of an alternative synthesis route that optimizes the metal dispersion of Mo with a high surface area of the support is required.

In a recently published article [24], ZrO_2 was impregnated on the surface of the Al_2O_3 in order to achieve a coating without phase separation between the ZrO_2 and Al_2O_3. The X-ray diffraction (XRD) results showed that ZrO_2 can be used up to a threshold coating of 15 nm without the formation of a ZrO_2 crystalline phase. Consequently, this synthesis method is very promising for the development of catalysts with a high dispersion of the active sites.

Therefore, based on this synthesis methodology which uti-

lizes an unconventional impregnation method combined with the polymeric precursor route, the present study shows the synthesis of catalysts containing MoO_3/Al_2O_3 using this alternative route and the influence of the addition of copper, iron, or nickel oxide on the catalytic properties for the dehydrogenation of ethylbenzene in the presence of CO_2. It is important to emphasize that catalysts containing molybdenum oxide supported on Al_2O_3 and doped with Fe, Ni, or Cu have been rarely reported in the literature for this reaction. Hence, the synthesis of new catalysts using this composition remains an interesting research topic. Furthermore, the role of molybdenum oxide in the reaction mechanism for the oxidative dehydrogenation of ethylbenzene and the influence of the dopant need to be clarified.

2. Experimental

2.1. Catalyst preparation

The sample of molybdenum oxide dispersed on Al_2O_3 was synthesized by the impregnation method. The Al_2O_3 used as support was the Degussa aeroxide particle with a surface area of 100 m^2/g (particle size estimated from isotherm data as 15 nm). However, before the impregnation process, the precursor source was prepared as a resin by the Pechini method containing Mo^{3+} ions using molybdic acid (Aldrich) [17].

The resin preparation involved the following steps. First, 26.49 g of the molybic acid solution was added to a beaker containing 200 mL of deionized water. This solution was kept under constant stirring at 80 °C for 3 h to obtain a MoO_4^{2-} suspension. Citric acid anhydride (J.T. Baker) was then added to complex the metallic ion, which gave a citric acid:Mo^{3+} complex with a metallic ion molar ratio of 3:1. The solution was kept under stirring at 80 °C for 48 h to promote the complexation process, after which 52.35 g of ethylene glycol was added and the solution was kept at 80 °C to perform the esterification and polymerization reaction.

Gravimetric analysis was carried out to determine the molybdenum oxide concentration in the resin. A quantity of resin that would result in the desired $MoO_3:Al_2O_3$ mass ratio was added to a beaker containing 150 mL of deionized water to coat the Al_2O_3. This system, with a viscosity similar to that of water, was stirred for 15 min and after that 1.0 g of Al_2O_3 was added. The resulting suspension was kept under constant stirring for 3 h at room temperature. It was then transferred to a round-bottomed flask, which was placed in a rotary evaporator to eliminate the water. The material obtained after evaporation of the water was calcined at 550 °C for 2 h with heating and cooling ramps of 10 °C/min. The synthesized sample has 10% by weight of molybdenum oxide on Al_2O_3. This sample was identified as 10MoAl. It is important to emphasize that the Mo^{3+} was added by an unusual way, since the molybdenum precursor (resin containing molybdenum) was added onto the Al_2O_3 support by the combination of a polymeric precursor route (Pechini) and wet impregnation on commercial Al_2O_3. This is in contrast to the normal method, which added directly an inorganic precursor as the molybdic acid onto the Al_2O_3 support.

Finally, the Ni, Cu, and Fe metals were added on the 10MoAl sample by the wet impregnation method. First, the nitrate salt of the metal (Ni, Cu, or Fe) was dissolved in 100 mL of distilled water and impregnated onto the 10MoAl solid under stirring and heating at 70 °C in a rotary evaporator until complete evaporation of the water. The resulting solid was calcined at 550 °C in air for 1 h and a ramp rate of 10 °C/min. These catalysts have a content of 2% by weight of the added oxide on the surface and are designated as 2CuMoAl, 2NiMoAl, and 2FeMoAl.

2.2. Catalyst characterization

XRD experiments were carried out on an XRD 600 (Shimadzu) using a Co K_α radiation source (λ = 0.1450 nm, 40 kV and 40 mA) with a wide angle diffraction pattern in the 2θ = 10°–80° range. Reference patterns from ICDD (International Centre for Diffraction Data) were used for the identification of the bulk phases.

The specific surface area (BET method), pore diameter, and pore volume of the catalysts were measured by N_2 adsorption-desorption isotherms at –196 °C on a Quantachrome Instruments Model Autosorb-1. The samples were first pretreated at 200 °C under vacuum (1.33 Pa).

The temperature of reduction was obtained by temperature-programmed reduction (H_2-TPR) analysis from 25 to 930 °C in a quartz reactor using a 8% H_2/N_2 mixture (25 mL/min) at a heating rate of 10 °C/min and 20 mg of the catalyst. A thermal conductivity detector was used to follow the H_2 consumption.

The oxidation of coke deposited during the catalytic tests was performed by thermogravimetric (TG) analysis with a Netzsch Model TG 209 F1 using a 10 °C/min heating rate under an air flow of 40 mL/min and 10 mg of sample.

2.3. Catalyst evaluation

Catalytic tests were carried out in a fixed-bed quartz microreactor using 100 mg of a sample at 550 °C and atmospheric pressure with a CO_2 to ethylbenzene molar ratio of 30. The molar flow rate of ethylbenzene was controlled to be 1.9×10^{-5} mol/min. Prior to the reaction, the catalyst was heated under a N_2 flow (30 mL/min) to the reaction temperature. The reaction mixture (CO_2, ethylbenzene, and N_2) was then introduced at a flow rate of 30 mL/min. The resulting catalytic ethylbenzene conversion was analyzed by gas chromatography using an instrument equipped with an FID and a nonpolar capillary column (30 mm × 0.25 mm × 0.25 mm, similar to AT-1). Heptane was used as the internal standard for the conversion and selectivity calculations from the chromatograms. The ethylbenzene conversion (C_{Et}) and the styrene selectivity (S_{St}) were calculated according to Eqs. (3) and (4), respectively:

$$C_{Et} = (ethylbenzene_{in} - ethylbenzene_{out})/ethylbenzene_{in} \quad (3)$$

$$S_{St} = styrene_{out}/n(hydrocarbon\ products) \quad (4)$$

All the obtained values were normalized by the internal standard.

3. Results and discussion

3.1. XRD results

In order to analyze the crystal structure formed after synthesis, the samples were subjected to XRD measurement. The results are present in Fig. 1.

The diffractograms presented the predominance of the Al_2O_3 phase with the tetragonal crystal system for all the samples (PDF-16-0394). Therefore, a high dispersion of the molybdenum oxide was suggested since no crystalline phase was observed for the molybdenum oxide. In addition, no nickel oxide, copper oxide, or iron oxide was observed. These characteristics are interesting for the catalytic process due to the high metal dispersion from the preparation method.

3.2. Surface area and porosity

The N_2 adsorption-desorption isotherms (Fig. 2) show the characteristic profiles of mesoporous materials for all the samples (type II isotherms according to the IUPAC classification). After the addition of the metal, Fe or Cu, the solid presented a hysteresis loop and consequently there was a change in the pore system of the material. This change was probably due to the re-calcination after the impregnation process with the nitrate, which was heated to decompose it, favoring the creation of pores produced from the liberation of nitrogen oxide gas during the thermal decomposition of the nitrate.

Table 1 presents the surface area, pore volume, and average pore diameter. The changes shown by the isotherms (Fig. 2) are now presented numerically. Mo addition resulted in a sample with a lower surface area compared to the pure Al_2O_3 support, which was increased after Ni, Cu, or Fe impregnation. However, no major change was observed in the textural properties of the catalysts with the variation of the composition. Thus, the addition of the Ni, Cu, or Fe metal by wet impregnation did not affect significantly the textural properties, substantially maintaining the characteristics of the Al_2O_3 support (S = 100 m²/g).
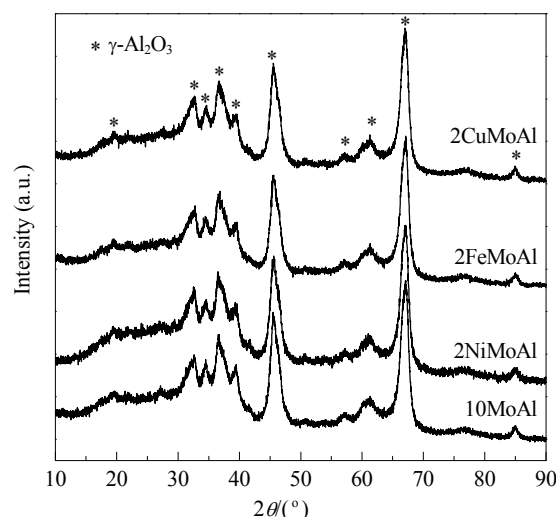

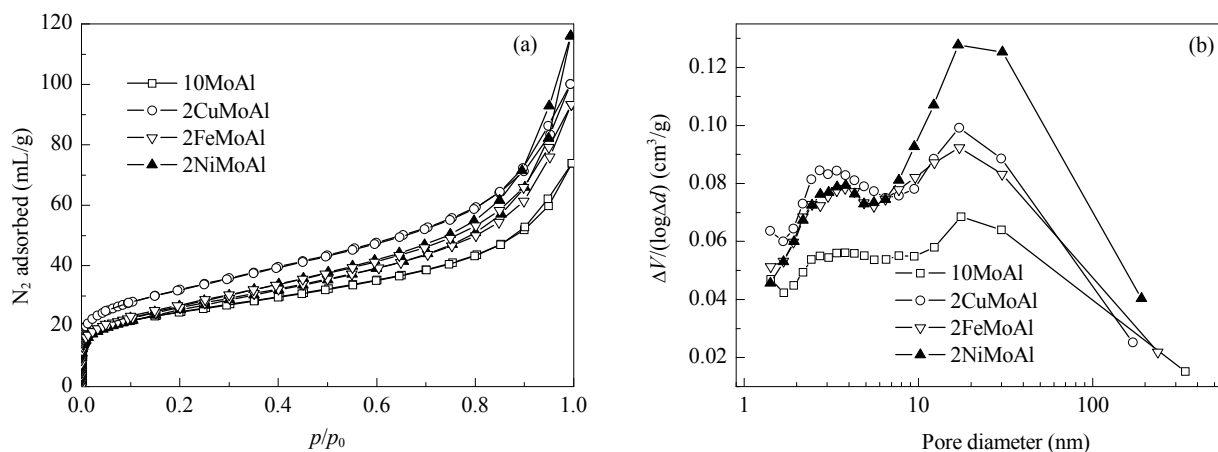**Fig. 1.** XRD patterns of the catalysts after calcination in air.

Fig. 2. N_2 adsorption-desorption isotherms (a) pore diameter distribution (b) of the samples.

Table 1
Textural properties of different catalysts.

Sample	S (m²/g)	V_p (cm³/g)	D_p (nm)
10MoAl	83	0.114	5.53
2NiMoAl	111	0.154	5.57
2FeMoAl	90	0.144	6.44
2CuMoAl	88	0.179	8.12

The maintenance of the surface area after impregnation and re-calcination would be interesting in the catalytic properties, especially if the active sites were well dispersed, which was suggested by the XRD results.

3.3. TPR results

TPR analysis was performed in order to observe the reducibility of the mixed metal oxides under a reducing atmosphere, and the influence of the transition metal (Ni, Fe, or Cu) on the 10MoAl structure. The results are presented in Fig. 3.

The TPR profile of the catalyst 10MoAl exhibited the reduction of the molybdenum oxide occurred in two stages. The first peak at low temperature (370–580 °C) with a maximum H_2 consumption at 470 °C can be attributed to the reduction of octahedral species. The high temperature peak (650–920 °C) can be associated with the partial reduction of tetrahedral species. It was reported that with a low amount of Mo, the molybdenum oxide was present mainly in the tetrahedral form due to the support effect. However, with intermediate amounts of Mo, such as the 10MoAl solid, both octahedral and tetrahedral species were present and were more easily reduced [25].

The 2NiMoAl sample presented three clear reduction bands. The first band in the range of 300 to 450 °C with the maximum at 410 °C is related to the reduction of molybdenum oxide and nickel oxide species, which act as a catalyst (nickel species) for Mo oxide partial reduction. The second reduction step (450–660 °C) with a maximum of H_2 consumption at 573 °C was assigned to the reduction of NiO species dispersed on the alumina surface, which presented a higher support effect. Finally, the third reduction range, higher than 660 °C, was asso-

ciated with reduction of molybdenum species in its tetrahedral form, consequently, the most difficult to reduce.

The 2FeMoAl sample presented a reduction profile similar to the 10MoAl solid with two reduction peaks with the maximum temperature at 480 and 810 °C, respectively. These two bands can be attributed to the two reduction steps of iron oxide, Fe^{3+} to Fe^{3+}/Fe^{2+} followed by reduction of Fe^{3+}/Fe^{2+} to Fe^0, respectively. However, this material presented broader and more intense bands compared to the 10MoAl sample. These results may be related to the reduction of the molybdenum and iron oxides, which occur in the same temperature range. Nevertheless, this material has a maximum reduction peak at 480 °C, which is slightly higher than the 10MoAl sample. Therefore, it was not possible to show the catalytic effect of iron oxide addition on the molybdenum oxide reduction.

It was already reported that the addition of MoO_3 to Fe_2O_3 inhibited the reduction of iron oxide to metallic iron [26]. This phenomenon was attributed to the polarization of the Fe–O bonds, promoted by the Mo^{+6} ions, resulting in a more ionic character, and consequently these were less reducible [26]. However, the profile presented by the 2FeMoAl sample did not show this phenomenon since the iron oxide content was small (2 wt%).

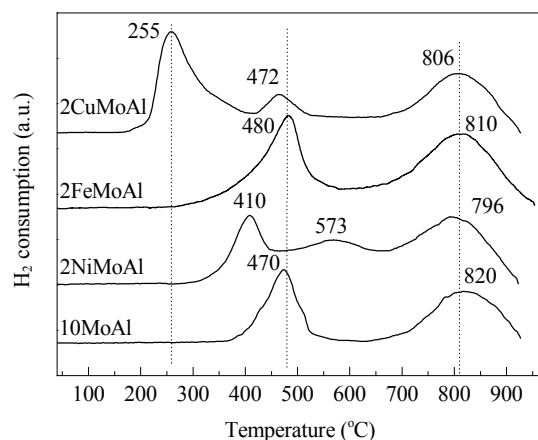However, the 2CuMoAl sample showed a reduction peak at

Fig. 3. H_2-TPR profiles of the catalysts.

lower temperature (255 °C) compared to the other solids, which was mainly due to the reduction of CuO to Cu^0. However, the reduction of MoO_3 octahedral species in this temperature range cannot be ruled out due to the Cu catalytic effect. It was observed that the phenomenon of MoO_3 reduction was more intense for materials containing copper oxide than the nickel oxide-based catalyst. In spite of the absence of data on the Cu, Ni, or Fe dispersion, it was suggested that there was a higher CuO distribution compared with the NiO species.

On the other hand, the reduction profiles for all the samples indicated that molybdenum oxides were well dispersed on the Al_2O_3 surface and interacted strongly with the dopant, which probably favor the catalytic process. It is known that a strong metal support interaction (SMSI) effect modifies the adsorption properties of a surface, modifying the ability to reduce/oxidize materials, consequently changing the catalytic performance [27–29]. It is important to highlight the fact that the redox and acid-base properties of the catalyst for the oxidative dehydrogenation of ethylbezene are very important, hence, the oxidation state of the active site (molybdenum oxide) and interaction with the other species (Ni, Cu, or Fe) would directly affect the catalytic performance.

3.4. Ethylbenzene dehydrogenation reaction

The ethylbenzene conversion and styrene selectivity results are presented in Fig. 4. The addition of small amounts of Ni, Fe, or Cu metal promoted the initial conversion since the undoped catalyst showed the lowest conversion compared to the other solids. The improvement in conversion with the addition of a dopant may be related to the high dispersion of these metals on the catalyst surface and the interaction between the added metal and support provided by the synthesis method employed as suggested by characterization results. However, clear differences in catalytic stability were observed during the 6 h of reaction since the 2NiMoAl material which had a higher initial conversion presented the worst performance at the end of the reaction compared to the other catalysts.

In spite of the smaller initial conversions of the 10MoAl catalysts, an unusual phenomenon for this reaction was a noticeable increase in the conversion during the first 60 min for these

two samples. This may be related to the oxide reduction process for these metals based on the fact that the dehydrogenation reaction leads to the formation of hydrogen (reducing atmosphere), which will cause the reduction of the oxide.

The ethylbenzene conversion results are in good agreement with the TPR results, which indicated that most of these oxides were reduced at temperatures below 550 °C (reaction temperature). This was confirmed by Moronta et al. [18] who studied the effect of reduction of Co and Mo bimetallic samples supported on pillared clays. These catalysts showed a higher activity when subjected to a reduction process. However, the formation of catalytic carbon deposit during the reaction, which also promotes an increase in conversion, despite being quite rare, cannot be neglected. It requires more detailed studies to confirm this assumption [30–32].

On the other hand, the 2FeMoAl and 2NiMoAl samples presented a more expected behavior for the catalysts used in this reaction because a deactivation was observed during the reaction, mainly for the 2NiMoAl material (36% deactivation). This process is possibly related to the carbon deposition and the reduction of oxides on the Al_2O_3 surface, which was well presented in the literature [14,15]. The higher initial acidity of the Ni species would give more cracking byproducts such as benzene. This would result in coke deposition on the solid surface leading to rapid deactivation [33]. All the samples showed styrene selectivity of 97% at the end of the process, except for the catalyst containing Ni. The 2NiMoAl solid presented a lower styrene selectivity (94%) and more benzene formation, corroborating the previous results.

It is important to emphasize that the conversion results presented in this work are interesting, especially for the 2CuMoAl and 2FeMoAl solids, as compared to the conversion values in the literature for catalysts containing molybdenum oxide [16–18,34].

The literature reports give a positive effect for the addition of dopants in the catalytic performance (activity, selectivity, and stability), which supports the results presented in Fig. 4. Several reasons are given for the promotional effect in the mixed oxide solids, which explained the best performance of the bimetallic samples compared to the monometallic: (1) the formation of a variety of varied valence simultaneously with
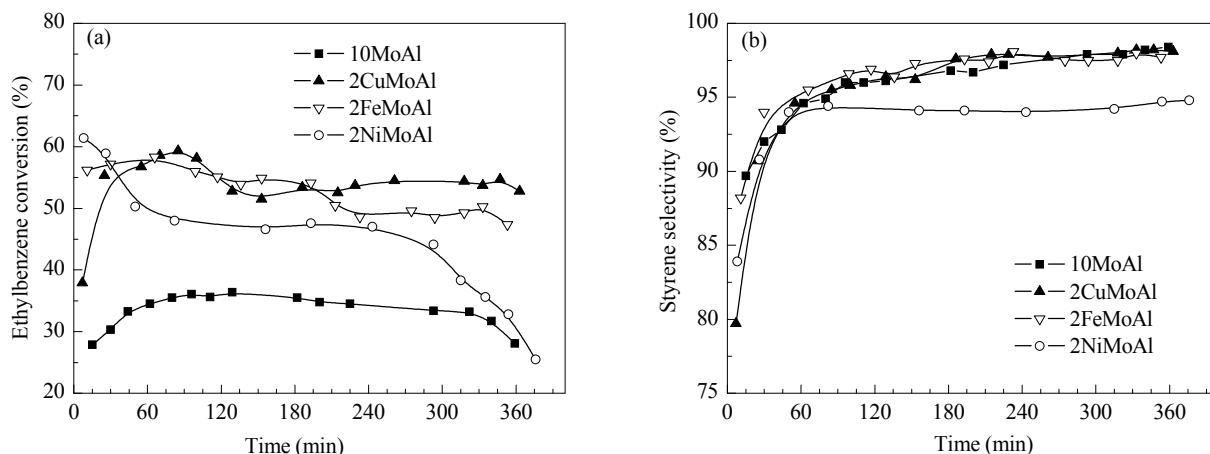

Fig. 4. Catalytic tests results at 550 °C for the unreduced catalysts. (a) Ethylbenzene conversion; (b) Styrene selectivity.

the alteration of the redox proprieties, favoring the reaction mechanism; (2) change of the reciprocal interaction between the active sites and consequently the weakening of the metal-oxygen bonds; (3) and the synergy effects between the phases, as observed in the TPR results [35–38].

The redox mechanism involves the adsorption and reduction of the catalyst by H_2 or CO, and oxidation of the catalyst by CO_2 and desorption [39]. The dehydrogenation process in the presence of CO_2 can be considered as two consecutive reactions: dehydrogenation followed by the reverse water gas shift (RWGS), or as a direct dehydrogenation by CO_2 [39].

Some papers support the formation of styrene from ethylbenzene by the redox mechanism using the lattice oxygen in the catalyst such as perovskites, iron oxide, vanadium oxide, etc. [39–41]. On the other hand, molybdenum oxide as an active center and its role in the oxidative dehydrogenation of ethylbenzene to styrene is rarely mentioned in the literature [42].

The redox and surface acid–base properties of Mo-based catalysts have been discussed to play an essential role in the partial oxidation of hydrocarbons such as ethane, propane, and ethylbenzene. During the oxidation reaction, lattice oxygen from molybdenum oxide oxidizes the hydrocarbon, leaving a reduced center that is reoxidized by the oxidizing agent (CO_2, H_2O, and O_2). It is also recognized that the adsorption and activation of the hydrocarbon molecules are associated with acid–base interactions, and the adsorption and desorption rates of products are correlated with the acid–base properties [42–44]. Thus, an active, selective, and stable solid containing molybdenum oxide needs to have a combination of acid–base and redox properties [43,44]. Molybdenum oxide may play a similar role in the oxidative dehydrogenation of ethylbenzene to styrene as compared to other traditional catalysts such as iron oxide.

In order to understand the unexpected behavior for 10MoAl and 2CuMoAl (Fig. 4), additional catalytic tests were carried out for the two samples. The catalysts were reduced in H_2 at 550 °C before the reaction. The ethylbenzene conversion and styrene selectivity results for the reduced materials are labeled in Fig. 5. Interestingly, in these new catalytic tests, a more common phenomenon was observed for this reaction because a re-

markable deactivation during the 6 h of reaction was seen. Comparing the initial conversion of the reduced catalyst (Fig. 4) with unreduced catalyst (Fig. 5), it was noticed that the initial conversion was much higher for the reduced solids. This explained the increase in conversion in the first minutes of reaction (Fig. 4) since for these two catalysts, the reduced species are more active than the unreduced. The styrene selectivity was similar for both types of pretreatment. The influence of the oxidation state of the active site on the catalytic performace and its influence on the redox mechanism have been described in the literature [17,18,36]. Hanuza et al. [42] showed that the oxidation state of the molybdenum oxide affected the reaction mechanism for the oxidative dehydrogenation of ethylbenzene and consequently the catalytic performance. Therefore, the addition of a dopant to optimize the redox and acid–base properties is essential to trigger the reaction mechanism.

3.5. Characterization after the catalytic tests

In order to better understand the observed results in the catalytic performance (Fig. 4), XRD and TG analysis were carried out after the catalytic tests for the unreduced catalysts. The XRD results are presented in Fig. 6. For 2CuMoAl, it was seen that there was the maintenance of the Al_2O_3 phase (PDF-16-0394), which was observed in Fig. 1. Furthermore, the presence of metallic copper was detected, confirming the reduction of CuO to Cu during the reaction. Thus, Cu is more active than CuO due to increased conversion in the first minutes (Fig. 4). The presence of Cu^0 had already been observed in the TPR profile (Fig. 3) because Cu is fully reduced at the chosen reaction temperature (550 °C). For the 2NiMoAl catalyst, beside the Al_2O_3, the formation of metallic nickel was noticed, corroborating the TPR results, because nickel is also completely reduced in the temperature range of the reaction.

On the other hand, for the 2FeMoAl and 10MoAl solids, it was observed that there was practically no change compared to the XRD results before the reaction (Fig. 1). However, the TPR results showed that iron and molybdenum could be partially reduced in the temperature range of the reaction. Thus, this is another indication that the synthesis method led to a high interaction between the species, as observed in the TPR results,
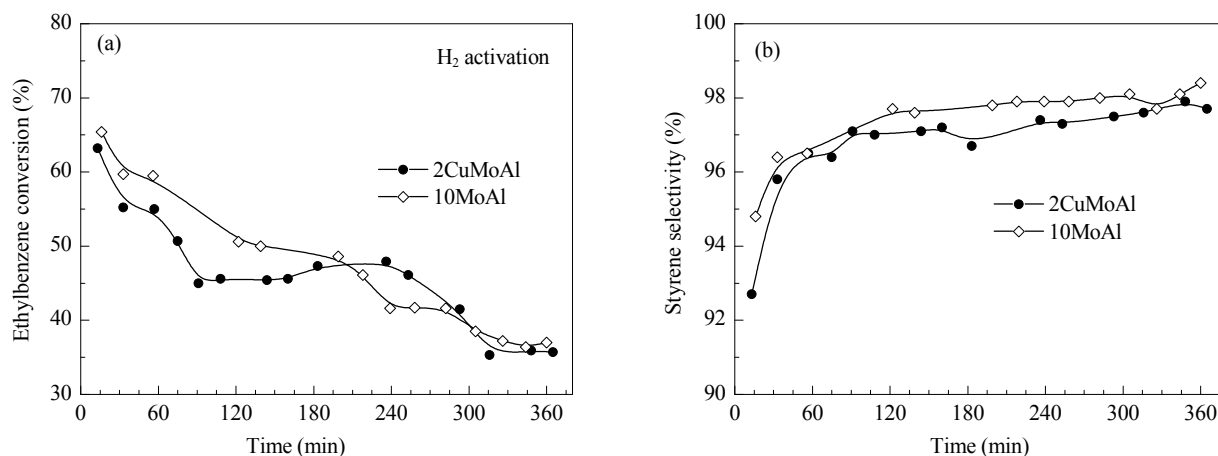

Fig. 5. Catalytic tests at 550 °C for the reduced solids 10MoAl and 2CuMoAl. (a) Ethylbenzene conversion; (b) Styrene selectivity.
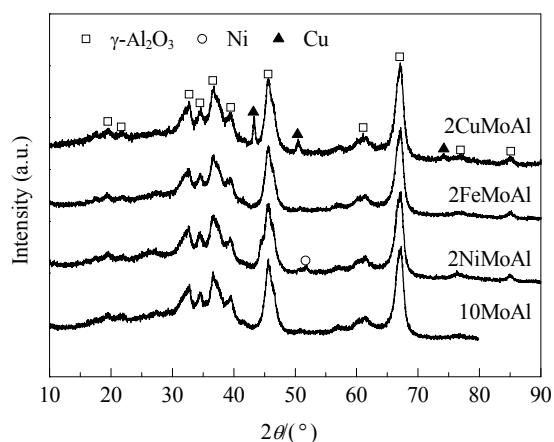
Fig. 6. XRD patterns for the samples after the catalytic test for the unreduced solids.

which resulted in the hindering of the sintering process and consequently favoring high dispersion of the species on the Al_2O_3 support and preventing their identification by XRD. The high dispersion of the iron species and its high interaction with the support (10MoAl) would explain its better catalytic conversion (Fig. 4).

The amount of carbon deposited on the catalyst surface during the reaction process was investigated by TG analysis (Fig. 7). It was observed that the sample with Ni (2NiMoAl) presented the highest amount of carbon deposited followed by 2CuMoAl, 10MoAl, and 2FeMoAl.

A larger amount of carbon deposited for the catalyst containing Ni was possibly due to its high acidity, which led to increased cracking byproducts, as noted in Fig. 4, and conse-

quently poorer catalyst stability (high deactivation rate) [33]. Therefore, the TG results after the catalytic tests aided in the interpretation of the catalytic performance because catalytic stability and styrene selectivity are directly related to the amount of carbon deposited on the solid surface.

Most of the catalysts exhibited a weight loss due to carbon oxidation in the low temperature region (between 300 and 500 °C), indicating the formation of carbon with a low molecular weight or low C/H ratio, or a carbon type which contains oxygen in its structure [15,32,33]. However, interestingly, the catalyst 2NiMoAl presented a second carbon burning region, which was possibly linked to the formation of crystalline carbon.

Zarubina et al. [33] showed the formation of oxygen-rich coke and polycondensed/aromatic coke from ethylbenzene dehydrogenation, which can provide an increase in conversion during the reaction (catalytic coke). Thus, the increase in conversion and styrene selectivity for the solids 2CuMoAl and 10MoAl due to the carbon deposited during the ethylbenzene dehydrogenation in the presence of CO_2 cannot be totally ruled out. However, this is extremely unlikely according to the catalytic tests of the reduced and unreduced samples (Figs. 4 and 5).

4. Conclusions

The catalysts synthesized using an alternate route gave interesting results in the catalytic ethylbenzene dehydrogenation reaction to styrene, making its investigation attractive. XRD results indicated that the metal dopants added by impregnation were well dispersed on the Al_2O_3 support. The addition of a metal dopant by wet impregnation did not affect the textural
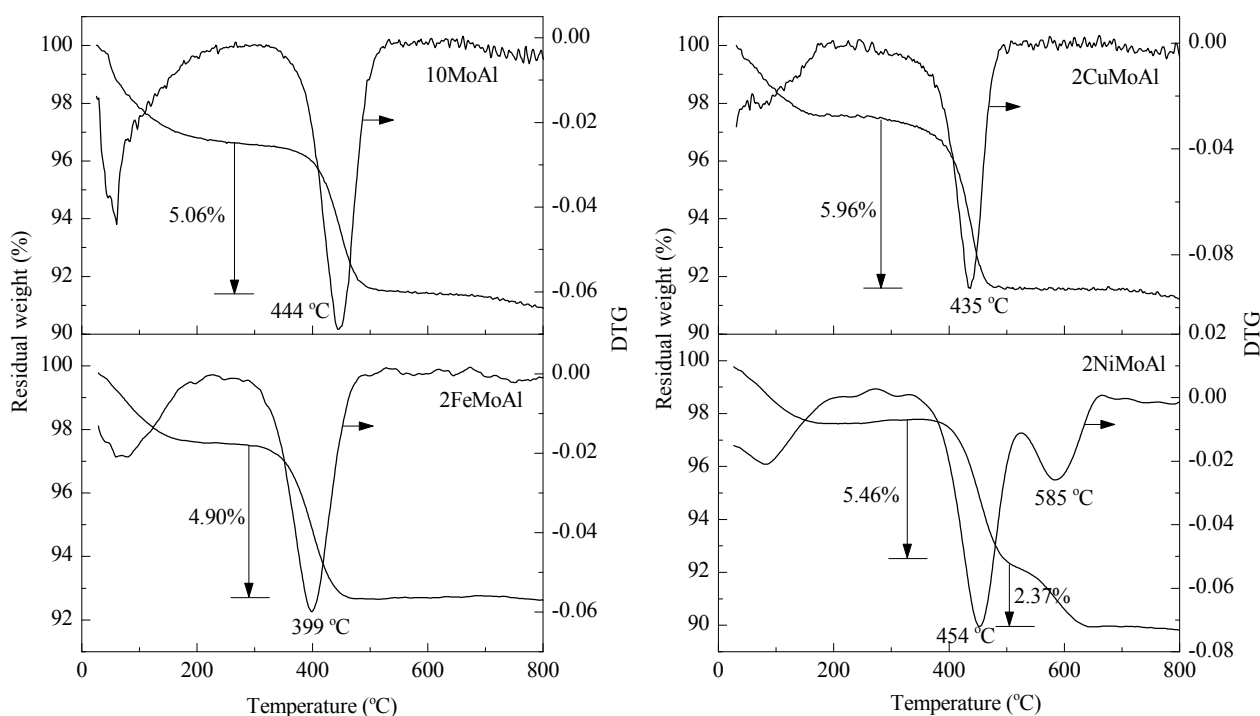

Fig. 7. TG curves of the samples after the catalytic test (6 h of reaction) for the unreduced catalysts.

properties of the support. TPR results indicated that there was an interaction between the metal dopant and molybdenum oxide. The addition of a dopant promoted the initial ethylbenzene conversion. The choice of the metal dopant affected the stability and selectivity during the first 6 h of reaction. The catalyst doped with copper demonstrated an increase in conversion during the first hour of time on stream. The 2CuMoAl and 10MoAl solids gave higher conversions when subjected to a reduction before reaction, indicating that the reduced species are more active than the unreduced solids. The Ni-based solid exhibited the largest amount of carbon deposited, explaining its rapid deactivation. Molybdenum oxide plays a crucial role in the oxidative dehydrogenation of ethylbenzene to styrene by its redox and acid–base properties. The addition of a dopant can promote the redox and acid–base properties, which are essential for the reaction mechanism. Further studies are necessary to reinforce the precise role of molybdenum oxide and the influence of the metal dopant.

Acknowledgments

References

[1] Baghalha M, Ebrahimpour O. *Appl Catal A*, 2007, 326: 143
[2] Hirano T. *Appl Catal*, 1986, 26: 65
[3] Mimura N, Saito M. *Catal Today*, 2000, 55: 173
[4] Park S E, Han S C. *J Ind Eng Chem*, 2004, 10: 1257
[5] Sun A L, Qin Z F, Wang J G. *Appl Catal A*, 2002, 234: 179
[6] Sakurai Y, Suzaki T, Ikenaga N, Suzuki T. *Appl Catal A*, 2000, 192: 281
[7] Sato S, Ohhara M, Sodesawa T, Nozaki F. *Appl Catal*, 1988, 37: 207
[8] Fedorov G I, Sibgatullin S G, Solodova N L, Izmailov R I. *Petrol Chem*, 1976, 16(3): 162
[9] Cavani F, Trifirò F. *Appl Catal A*, 1995, 133: 219
[10] Li C G, Miao C X, Nie Y Y, Yue Y H, Gu S Y, Yang W M, Hua W M, Gao Z. *Chin J Catal*, 2010, 31: 993
[11] Li H Y, Yue Y H, Miao C X, Xie Z K, Hua W M, Gao Z . *Chin J Catal*, 2006, 27: 4
[12] Ikenaga N, Tsuruda T, Senma K, Yamaguchi T, Sakurai Y, Suzuki T. *Ind Eng Chem Res*, 2000, 39: 1228
[13] Carja G, Nakamura R, Aida T, Niiyama H. *J Catal*, 2003, 218: 104
[14] He X X, Fan C, Gu X Y, Zhou X G, Chen D, Zhu Y A. *J Mol Catal A*, 2011, 344: 53
[15] Braga T P, Pinheiro A N, Teixeira C V, Valentini A. *Appl Catal A*, 2009, 366: 193
[16] Wong S T, Lin H P, Mou C Y. *Appl Catal A*, 2000, 198: 103
[17] Morán C, González E, Sánchez J, Solano R, Carruyo G, Moronta A. *J Colloid Interface Sci*, 2007, 315: 164
[18] Moronta A, Troconis M E, González E, Morán C, Sánchez J, González A, Quinónez J. *Appl Catal A*, 2006, 310: 199
[19] Pramod C V, Raghavendra C, Reddy K H P, Babu G V R, Rao K S R, Raju B D. *J Chem Sci*, 2014, 126: 311
[20] Su X Y, Wang R, Su D S. *Chin J Catal*, 2013, 34: 508
[21] Chen D, Holmen A, Sui Z J, Zhou X G. *Chin J Catal*, 2014, 35: 824
[22] Cavani F, Trifiro F. *Appl Catal A*, 1995, 133: 219

Graphical Abstract

Chin. J. Catal., 2015, 36: 712–720   doi: 10.1016/S1872-2067(14)60313-2

Cu, Fe, or Ni doped molybdenum oxide supported on Al₂O₃ for the oxidative dehydrogenation of ethylbenzene

Tiago Pinheiro Braga*, Antônio Narcísio Pinheiro, Edson R. Leite, Regina Cláudia R. dos Santos, Antoninho Valentini
Federal University of Rio Grande do Norte, Brazil; Federal University of Ceará, Brazil; Federal University of São Carlos, Brazil
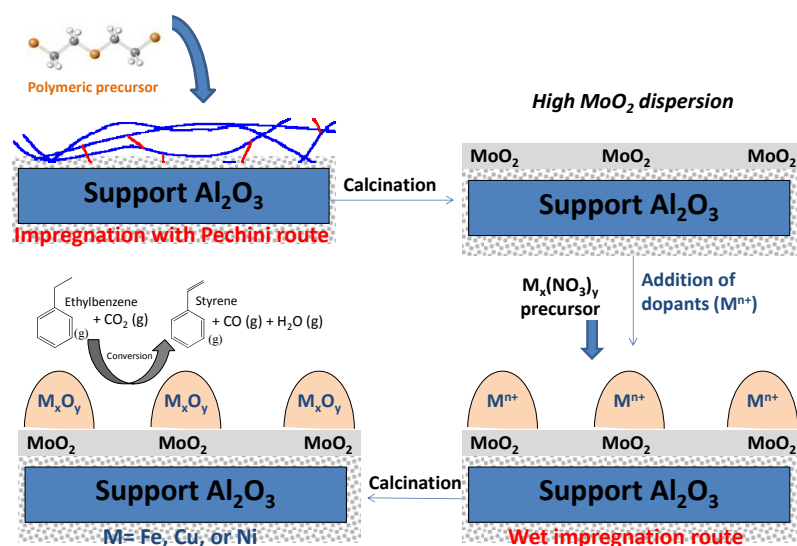
Molybdenum oxide was supported by an unusual way: the molybdenum precursor (resin containing molybdenum) was added onto the alumina support by the combination of the polymeric precursor route (Pechini) and wet impregnation on commercial Al₂O₃.

[23] Xin Q, Lin L W. *Chin J Catal*, 2013, 34: 401

[24] Dalmaschio C J, Mastelaro V R, Nascente P, Bettini J, Zotin J L, Longo E, Leite E R. *J Colloid Interface Sci*, 2010, 343: 256

[25] Chary K V R, Reddy K R, Kishan G, Niemantsverdriet J W, Mestl G. *J Catal*, 2004, 226: 283

[26] Al-Shihry S S, Halawy S A. *J Mol Catal A*, 1996, 113: 479

[27] Humblot F, Candy J P, Le Peltier F, Didillon B, Basset J M. *J Catal*, 1998, 179: 459

[28] Kaneko S, Arakawa T, Ohshima M, Kurokawa H, Miura H. *Appl Catal A*, 2009, 356: 80

[29] Men Y, Yang M. *Catal Commun*, 2012, 22: 68

[30] Delgado J J, Chen X, Tessonnier J P, Schuster M E, Del Rio E, Schlögl R, Su D S. *Catal Today*, 2010, 150: 49

[31] Nederlof C, Kapteijn F, Makkee M. *Appl Catal A*, 2012, 417-418: 163

[32] Zarubina V, Nederlof C, Van der Linden B, Kapteijn F, Heeres H J, Makkee M, Melian-Cabrera I. *J Mol Catal A*, 2014, 381: 179

[33] Braga T P, Sales B M C, Pinheiro A N, Herrera W T, Baggio-Saitovitch E, Valentini A. *Catal Sci Technol*, 2011, 1: 1383

[34] Pochamoni R, Narani A, Gurram V R B, Gudimella M D, Potharaju P S S P, Burri D R, Rao K S R. *Indian J Chem Sect A*, 2014, 53A: 493

[35] Oganowski W, Hanuza J, Drulis H, Mista W, Macalik L. *Appl Catal A*, 1996, 133: 143

[36] Irún O, Sadosche S A, Lasobras J, Soler J, Francés E, Herguido J, Menéndez M. *Catal Today*, 2013, 203: 53

[37] Park M S, Vislovskiy V P, Chang J S, Shul Y G, Yoo J S, Park S E. *Catal Today*, 2003, 87: 205

[38] Abello M C, Gomez M F, Ferretti O. *Appl Catal A*, 2001, 207: 421

[39] Nederlof C, Talay G, Kapteijn F, Makkee M. *Appl Catal A*, 2012, 423-424: 59

[40] Watanabe R, Sekine Y, Kojima J, Matsukata M, Kikuchi E. *Appl Catal A*, 2011, 398: 66

[41] He X X, Fan C, Gu X Y, Zhou X G, Chen D, Zhu Y A. *J Mol Catal A*, 2011, 344: 53

[42] Hanuza J, Jezowska-Trzebiatowska B, Oganowski W. *J Mol Catal*, 1978, 4: 271

[43] Abello M C, Gomez M F, Ferretti O. *Appl Catal A*, 2001, 207: 421

[44] Vedrine J C, Millet J M M, Volta J C. *Catal Today*, 1996, 32: 115